

## Chapter 4

# BIOACTIVITY AND MECHANICAL BEHAVIOR OF CERIUM AND LANTHANUM SUBSTITUTED BIOACTIVE GLASS AND ITS CERAMIC DERIVATIVES

---

### 4.1 Introduction

45S5 bioactive glasses have been widely investigated for bone repair because of their excellent bioactive properties. However, bioactive materials undergo incomplete conversion into a bone-like material which has biomedical application [L.L. Hench, 1991]. In simulated body fluid (SBF), bioactive glasses bind to living bone through an apatite layer formed on their surfaces [M. Bohner et al. 2009]. Bioactive material should possess excellent biochemical behavior and biomechanical strength. The 45S5<sup>®</sup> bioactive glass has very good capability to bond with both the soft and hard tissues [L.L. Hench et al. 1993]. Hench decided to make a glass of the SiO<sub>2</sub>-Na<sub>2</sub>O-CaO-P<sub>2</sub>O<sub>5</sub> system containing high calcium contents with a composition close to a ternary eutectic in the Na<sub>2</sub>O-CaO-SiO<sub>2</sub> diagram [L.L. Hench et al. 2006]. The main discovery was that a glass of the mol% composition 46.1 SiO<sub>2</sub>-24.4 Na<sub>2</sub>O-26.9 CaO-2.6 P<sub>2</sub>O<sub>5</sub>, known as 45S5 bioglass, formed a strong bond with bone which could not be removed without breaking the bone [L.L. Hench et al. 1971]. This launched the field of bioactive ceramics with many new materials and products [T. Kokubo. 1991]. Substitution of bioactive glasses with different transition and rare earth metals such as cerium, lanthanum, zinc, manganese, iron, magnesium and silver to change their biological and bioactive response has been studied by a number of research groups [R. Z. Legeros et al, 2002; J.R. Jones et al. 2006]. A biomaterial is a

synthetic material to be used in intimate contact with living tissue. In this work we study the effect of CeO<sub>2</sub> doping on the thermal, optical, mechanical and in vitro properties of the bioactive glass. Ce ions have been used in dental ceramics to mimic the fluorescence of natural teeth [J.L. Rygel et al. 2009]. Cerium is also known to possess bacteriostatic properties and has low toxicity [C. Leonelli et al. 2003]. The 45S5 bioactive glass is a very successful biomaterial for clinical applications and many researchers have studied with an incorporation of some ions such as Li, Zn, Ti, K, Zr, Mg, Fe, and Sr in the base bioactive glass because of their unique outcome on osteoblastic cell proliferation of different ions in the base bioactive glasses [S.K. Arepalli et al. 2015]. The present work is concerned with the preparation and characterization of cerium and lanthanum containing Bioactive Glass (BG). These bioactive glasses were immersed in simulated body fluid (SBF) to validate the formation of a bone-like apatite layer on their surfaces by using FTIR. Surface morphology was studied using Scanning electron microscopy (SEM) and Mechanical properties were also studied.

## **4.2 Materials and methods**

### **4.2.1 Preparation of the bioactive glass composition**

The weight % compositions and ratio of CeO<sub>2</sub> to La<sub>2</sub>O<sub>3</sub> of the 45S5 bioglass samples have been given in Table 4.1. Fine-grained quartz was used as a source of SiO<sub>2</sub>. Analytical reagent grades CaCO<sub>3</sub>, Na<sub>2</sub>CO<sub>3</sub> and (NH<sub>4</sub>)H<sub>2</sub>PO<sub>4</sub> were used as a source of CaO, Na<sub>2</sub>O and P<sub>2</sub>O<sub>5</sub>, respectively. The required amounts of analytical reagent grade CeO<sub>2</sub> and La<sub>2</sub>O<sub>3</sub> were added one by one in the batch given in Table 4.1, for the partial substitution of SiO<sub>2</sub>. The raw materials for different samples were properly weighed. Then the mixing of different batches was done for 30 min and after that, they were melted in a 100 ml alumina crucible at 1400±5 °C in the

air as furnace atmosphere. The temperature of the furnace was controlled within  $\pm 10$  °C by an automatic temperature indicator controller. Glasses were melted at 1400 °C for 2 hours in an electric furnace with air as the furnace atmosphere for  $10$  °C  $\text{min}^{-1}$ . The melted samples were poured on a preheated aluminum sheet and directly transferred to a regulated muffle furnace at 520 °C for annealing.

**Table 4.1. Batch composition for  $\text{SiO}_2\text{-Na}_2\text{O-CaO-P}_2\text{O}_5\text{-CeO}_2\text{-La}_2\text{O}_3$  bioglass.**

Sample Id	Wt%					
	SiO <sub>2</sub>	Na <sub>2</sub> O	CaO	P <sub>2</sub> O <sub>5</sub>	CeO <sub>2</sub>	La <sub>2</sub> O <sub>3</sub>
BG	45	24.5	24.5	6	0.0	0.0
Ce-1	44.5	24.5	24.5	6	0.5	0.0
Ce-2	44	24.5	24.5	6	1.0	0.0
La-1	44.5	24.5	24.5	6	0.0	0.5
La-2	44	24.5	24.5	6	0.0	1.0

### 4.3 Results and discussions

#### 4.3.1 Differential thermal analysis (DTA) of substituted bioactive glass

The DTA plots of base bioactive glass and  $\text{CeO}_2\text{-La}_2\text{O}_3$  substituted glasses are shown in Figure 4.1. The DTA patterns of all the cobalt doped bioactive glass samples (Ce-1, Ce-2 La-1 and La-2) are similar to each other with respect to 45S5 bioactive glass in overall range of temperature. The bioactive glass sample (Ce-1) contain cerium oxide for silica in the glass as such its DTA pattern might be slightly different from 45S5 bioactive glass like others in the temperature range of 150-700°C but it resembles the patterns of other lanthanum oxide containing bioactive glasses as evident from DTA curves Figure 4.1. Tg value for the bioactive glass sample no Ce-1 has been clearly determined from its DTA curve as nucleation temperature from 541 to 538 °C and the crystallization temperature

from 690 to 570 °C. The DTA curves have shown only one exothermic peak corresponding to crystallization of a single phase in the bioactive glass-ceramic samples. The DTA curve shows the decrease in exothermic as well as endothermic peaks. This decrease in the peaks is due to incorporation of cerium and lanthanum oxide which might have entered the glass network and formed Si-O-Ce and Si-O-La bonds replacing the stronger Si-O-Si bonds. Thus the glass network becomes weaker and,  $T_g$  and  $T_c$  decreased [Azevedo et al. 2012]. Differential scanning calorimetry (DSC) performed by the authors for their non-charge balance (NonCB) bioactive glass samples had also shown that the glass transition temperature ( $T_g$ ) decreased with addition of  $Ce^{4+}$  ion upto 2.0 wt%  $CeO_2$  in a concentration dependent manner and further addition of  $La_2O_3$  upto 2 wt% decrease in  $T_g$  point of glass. As  $T_g$  decreased abruptly, the DSC data suggested that  $CeO_2$  has acted as a glass network intermediate oxide in smaller amounts whereas an increase in  $T_g$  with concentration of  $La_2O_3$  beyond 2.0% showed that  $La^{3+}$  ion acted as a glass network modifier upto 2 wt% in the NonCB bioactive glass.

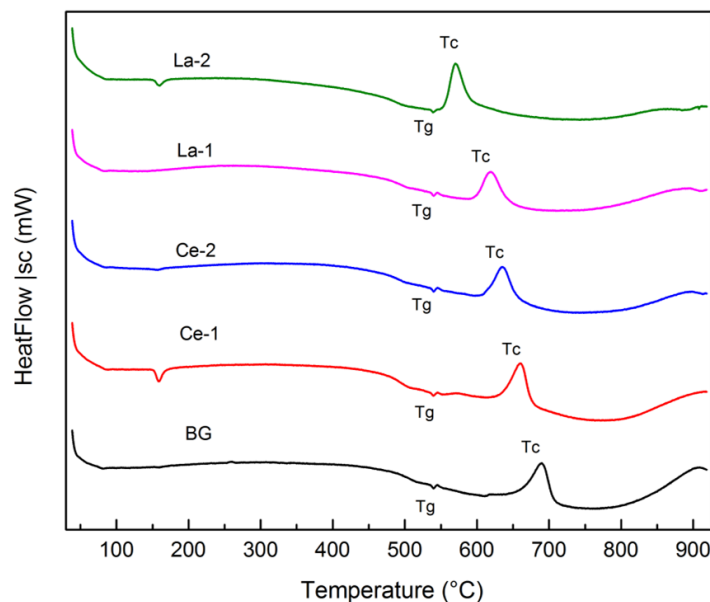


**Figure 4.1:** DTA Curve 45S5 bioactive glass substituted with Ce-La oxide.

### 4.3.2. XRD analysis of substituted bioactive glass

X-ray diffraction is a versatile, non-destructive technique that reveals comprehensive information about the chemical composition and crystallographic structure. In the XRD patterns, no peaks are found that's why all given bioglass samples are amorphous in nature.

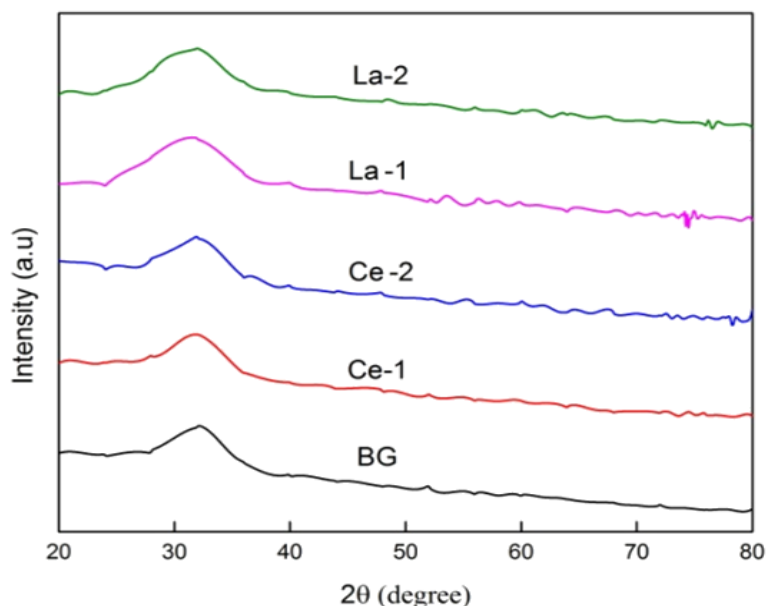


**Figure 4.2:**XRD patterns of the Ce-La substituted bioactive glass samples.

The XRD pattern of the powdered glass samples shows that there was no XRD peak for the glass. It shows that all the  $\text{SiO}_2\text{-Na}_2\text{O-CaO-P}_2\text{O}_5$  and Ce-La doped glass samples have been melted properly and converted into glassy solids.

### 4.3.3 FTIR assessment

The FTIR spectra of bioglass are presented in Figure 4.3 before soaking in SBF and Figure 4.4 after soaking for 13 days in SBF. Since there was a part of hydroxyapatite in the composition of prepared samples, it was expected to find the hydroxyl group peaks at  $3356\text{ cm}^{-1}$ .

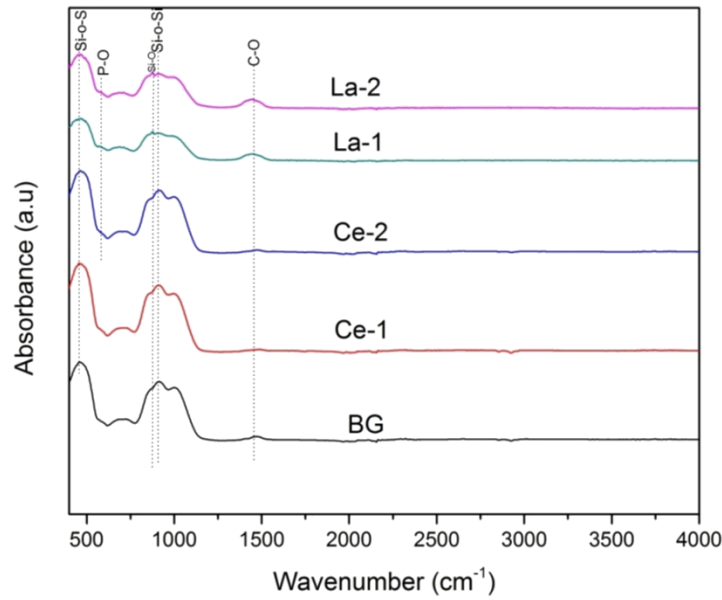


Figure 4.3: FTIR absorbance spectra of substituted glass samples before SBF solutions

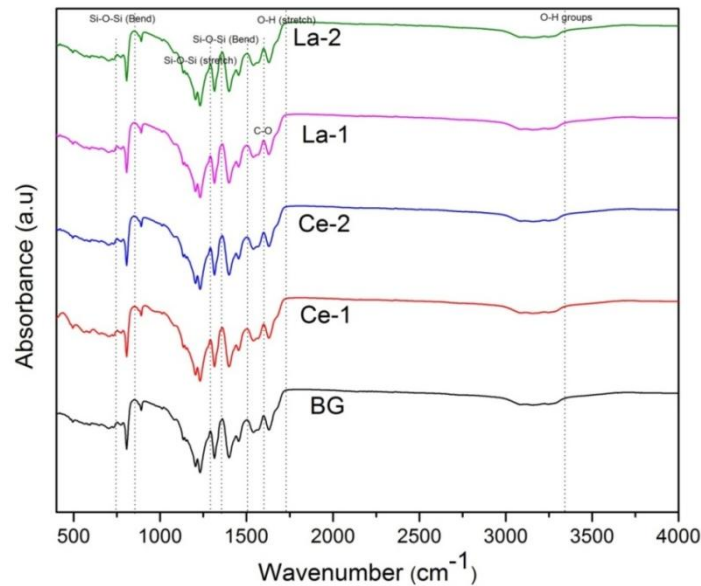
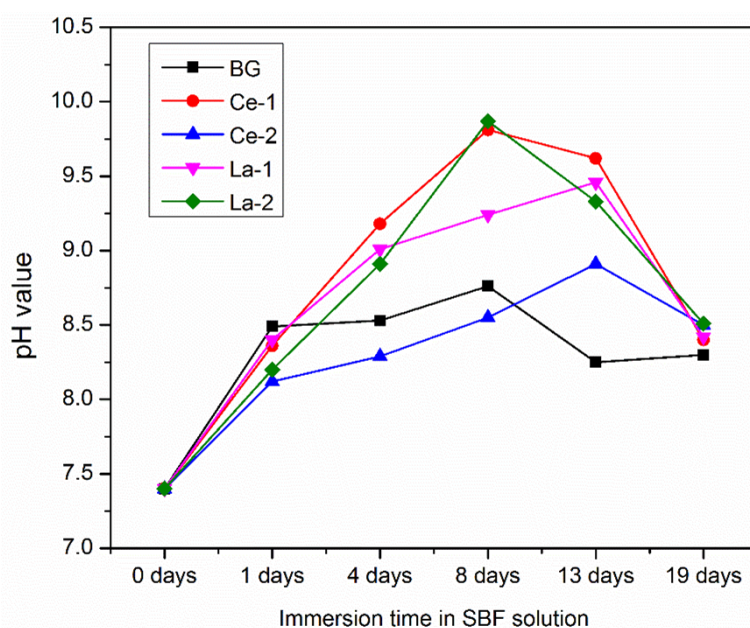


Figure 4.4: FTIR absorbance spectra of substituted bioglass samples after soaking in SBF for 13 days

#### 4.3.4 pH behavior in SBF

Figure 4.5, shows the variation of pH of bioactive glass samples after immersing in SBF solution up to 19 days. It shows that for all bioactive glass samples, the pH increases within 1–3 days as compared to the initial pH of the SBF solution at 7.4 under normal temperature and pressure conditions. The increase in pH values is due to fast release of cations through exchange with H<sup>+</sup> or H<sub>3</sub>O<sup>+</sup> ions in the SBF

solution. The  $H^+$  ions are being replaced by cations which cause an increase in hydroxyl concentration of the solution [F.H. El Batal et al. 2008]. This leads to attack on the silica glass network, which results in silanols formation leading to decrease in pH after 3 days as indicated when bioactive glass samples were immersed in SBF solution up to 19 days. The change in pH was due to leaching of cations. The increase in pH of SBF solution shows an increase in the concentration of  $H^+$  ions due to the replacement of cations in the bioactive glasses [L.L. Hench et al. 1971]. The maximum pH value is 9.87 of glass sample 1.0 weight %  $La^{3+}$  ion containing bioactive glass for 8 days in SBF solution.



**Figure 4.5:** Variation of pH of bioactive glass samples after immersing in SBF up to 19 days.

#### **4.3.5 Surface morphology of bioactive glass samples by SEM**

The surfaces morphology of bioactive glasses was analyzed before and after immersion in SBF solution by SEM. The samples were gold coated before SEM analysis. SEM (Inspect 50 FEI) was used for determining the surface microstructure of bioactive glass samples shown in Figure 4.6. When the bioglass sample were immersed in SBF solution for different time period then

Hydroxycarbonate apatite (HCA) layer was formed on the surface of bioactive glass samples in Figure 4.7.

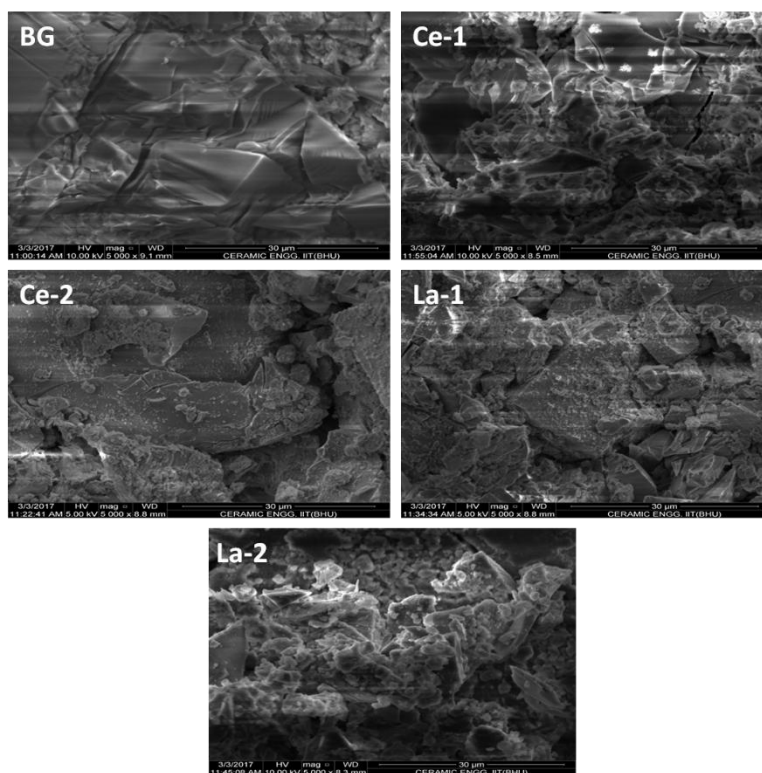


**Figure 4.6:** SEM of bioactive glasses BG, Ce-1 Ce-2, La-1 and La-2 before immersion in SBF respectively

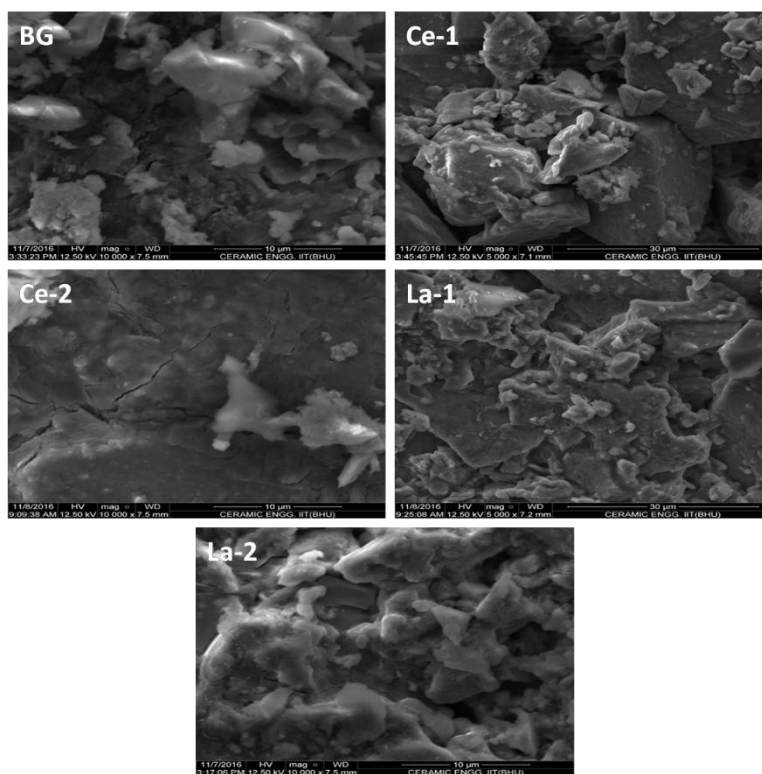


**Figure 4.7:**SEM of bioactive glasses BG, Ce-1 Ce-2, La-1 and La-2 after 19 days immersion in SBF solution

## 4.4 Mechanical properties

### 4.4.1 Density, flexural strength and microhardness

Figure 4.8 shows the density of the glass samples as a function of  $\text{CeO}_2/\text{La}_2\text{O}_3$  within error bars. It is clear that an increase in  $\text{CeO}_2/\text{La}_2\text{O}_3$  ratio by replacing  $\text{SiO}_2$  shows increase in the density of glass samples from 2.69 to 2.72 g/cc respectively. This is attributed due to the reason that the Cerium ions might have occupied interstitial sites within the glass network [M.R. Filgueiras et al. 1993; I. Rehman et al. 2000]. Therefore, it increased the densities and resulted in creating new bonds with incorporation of lanthanum ions in the bioactive glasses. It has caused reinforcement of glass structure and resulted in improvement in the compression of the glass samples.

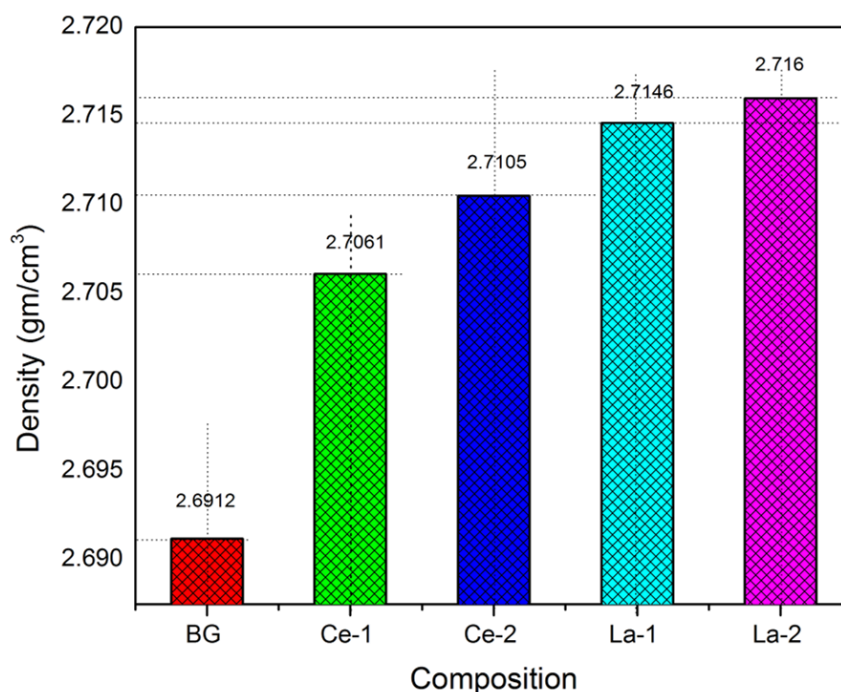


**Figure 4.8:** Density of BG, Ce-1 Ce-2, La-1 and La-2 substituted bioactive glass.

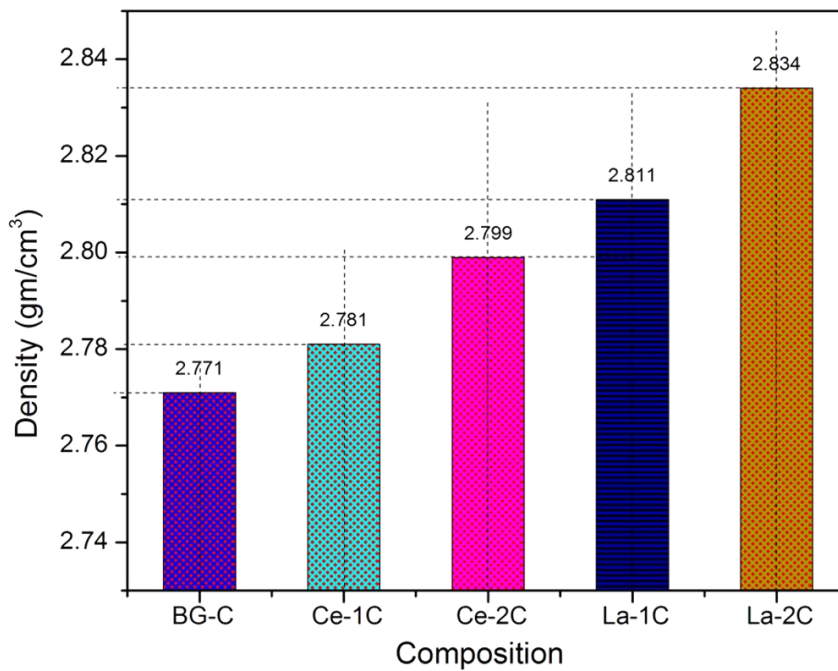
**Table 4.2:** Value of density ( $\text{gm/cm}^3$ ) of substituted bioglass and glass-ceramics.

Samples(Glass)	(BG)	Ce-1	Ce-2	La-1	La-2
Density( $\text{gm/cm}^3$ )	2.691	2.706	2.71	2.714	2.716

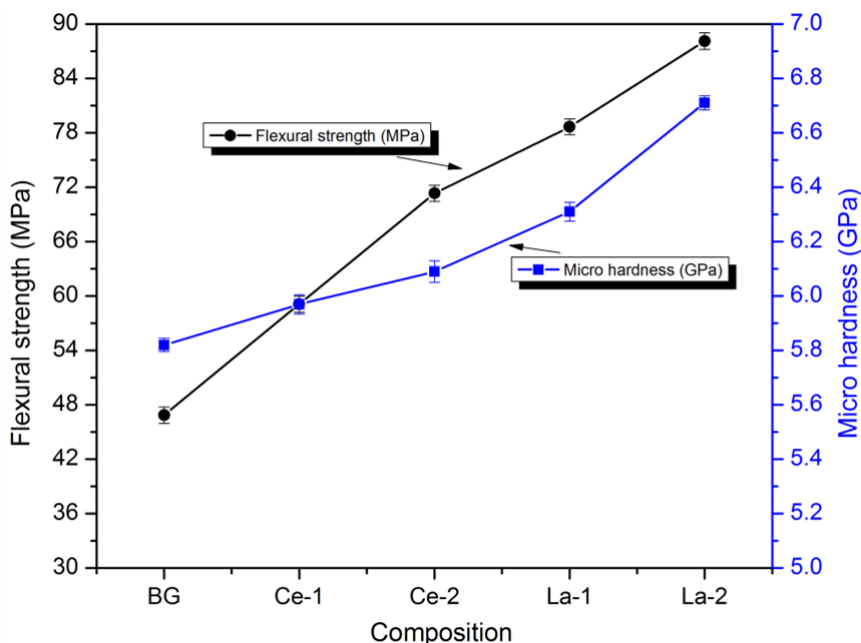
  

Samples (Glass Ceramics)	(BG)	Ce-1C	Ce-2C	La-1C	La-2C
Density( $\text{gm/cm}^3$ )	2.771	2.781	2.779	2.811	2.834

Figure 4.9 shows the density of cerium and lanthanum substituted 45S5 bioactive glass-ceramic which was measured by Archimedes' principle. It was observed that the densities of the samples have increased with increasing RRE's oxides content from 2.77 to 2.83  $\text{gm/cm}^3$  for glass-ceramics, respectively. It was found that  $\text{Ce}^{4+}$  and  $\text{La}^{3+}$  act as a glass network intermediate which increase the compactness of glass structure [A. Shrivastava et al. 2012].



**Figure 4.9:** Density of BG-C, Ce-1C Ce-2C, La-1C and La-2C substituted bioactive glass ceramics samples.



**Figure 4.10:** Flexural strength and Micro hardness of base bioactive glass and BG, Ce-1 Ce-2, La-1 and La-2 substituted bioactive glass.

**Table 4.3: Corresponding values of Micro hardness (GPa) and Flexural strength (MPa) of substituted bioactive glass**

Samples	45S5 (BG)	Ce-1	Ce-2	La-1	La-2
Micro hardness (GPa)	5.82	5.97	6.09	6.31	6.71
Flexural strength (MPa)	46.872	59.115	71.339	78.672	88.127

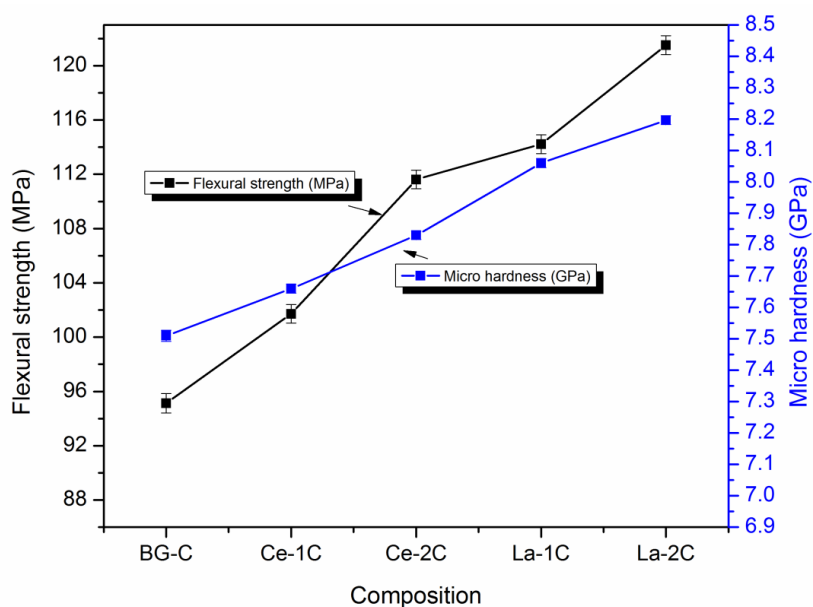


**Figure 4.11:** Flexural strength and Micro hardness of base bioactive glass and BG-C, Ce-1C Ce-2C, La-1C and La-2C substituted bioactive glass.

#### **4.4.2 Elastic modulus, shear modulus and bulk modulus and Poisson's ratio**

Figure 4.12 represents the experimental values of young's modulus (E), shear modulus (S) and bulk modulus (K) of the bioactive glass samples with increasing CeO<sub>2</sub> /La<sub>2</sub>O<sub>3</sub> ratio. All the elastic moduli values were found to increase with increasing CeO<sub>2</sub> -La<sub>2</sub>O<sub>3</sub> but Poisson's ratio decreases with the same content. The elastic moduli of the bioactive glass samples show similar trends regarding improvement in their mechanical properties with the variation in the ultrasonic velocities. The elastic modulus of alkali silicate glasses was normally found to increase with increasing concentration of modifier above a critical limit as a result of an increase in cohesion [S. Satoshi Hayakawa et al. 1999]. Thus, a greater bulk modulus of the glass samples can be partially attributed due to addition of more amounts of modifiers like CaO in the silicate glass samples. The authors have further mentioned that the effect of P<sub>2</sub>O<sub>5</sub> on the elasticity of their glasses was not clear, although phosphorus has caused a more polymerized silicate network. Hench [T. Kasuga et al. 2001] has pointed out that the Young's modulus of cortical bone is about 7–30 GPa which is far below then ostceramic based implants. Hence, from the point of view of biomechanical compatibility, the SiO<sub>2</sub>–CaO–P<sub>2</sub>O<sub>5</sub>–Na<sub>2</sub>O–CeO<sub>2</sub>–La<sub>2</sub>O<sub>3</sub> bioactive glass samples have been found to be better. It was also known that the glasses and ceramics are brittle materials, as a consequence of which their handling and mechanical properties are not adequate for significant load bearing applications. Therefore, a bioactive glass having elastic modulus higher than that of bone is required for medical applications. So, there was an increase in Young's modulus from 76.36 to 78.89 GPa with increasing CeO<sub>2</sub>/La<sub>2</sub>O<sub>3</sub> content in the present base bioactive glass. Similar results were also obtained for shear modulus and bulk modulus which showed

improvement in the mechanical properties of bioactive glasses with varying ultrasonic velocities.

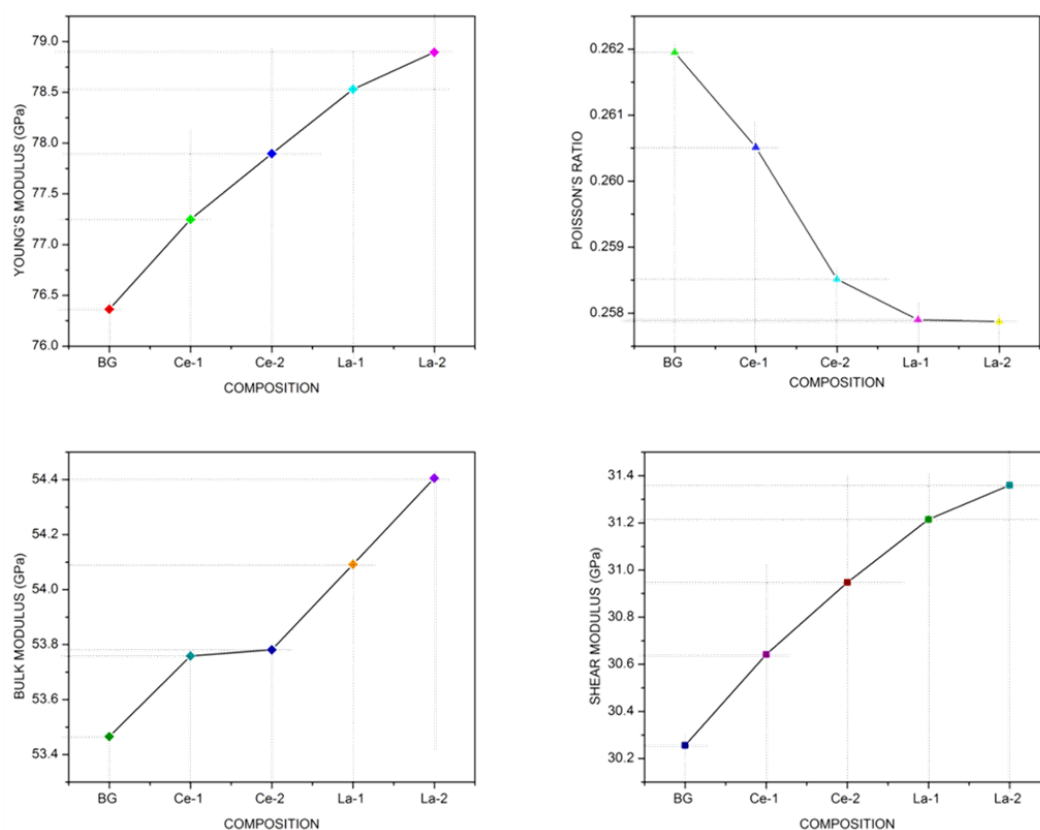


**Figure 4.12:** Young's modulus (E), Poisson's ratio, Shear modulus (S) and Bulk modulus (K) of the BG, Ce-1, Ce-2, La-1 and La-2 substituted bioactive glass samples.

## 4.5 Conclusions

In the present work, a comparative study was made on bioactive, physico-chemical and mechanical properties of multi-component  $\text{SiO}_2\text{-Na}_2\text{O-CaO-P}_2\text{O}_5\text{-CeO}_2\text{-La}_2\text{O}_3$  bioactive glasses with varying concentration of  $\text{CeO}_2$  and  $\text{La}_2\text{O}_3$ . The following conclusions were drawn from these investigations:

The results show that Young's, shear and bulk modulus increase with increasing concentration of rare earth oxides in non-charge balance (NCB) glass whereas the Poisson's ratio decrease with increasing concentration of same oxides. In addition of  $\text{Ce}^{4+}$  and  $\text{La}^{3+}$  ions was found that physical properties as well as

biological properties increased with increasing concentration of these rare earth ions. XRD pattern of modified 45S5 glass shows amorphous phase behaviour in presence of  $Ce^{4+}$  and  $La^{3+}$  ions. In FTIR spectra, Hydroxycarbonate apatite (HCA) layer is present after the immersion in SBF solution.

